

# DEVELOPMENT OF METALLIC HOT GAS FILTERS

I. E. Anderson

Metal & Ceramic Sciences Program, Ames Laboratory (USDOE),  
Iowa State University, Ames, IA. 50011, USA

E-mail: [andersoni@ameslab.gov](mailto:andersoni@ameslab.gov); Telephone: (515) 294-9791; FAX: (515) 294-8727

B. Gleeson

Metal & Ceramic Sciences Program, Ames Laboratory (USDOE),  
Iowa State University, Ames, IA. 50011, USA

E-mail: [bgleeson@ameslab.gov](mailto:bgleeson@ameslab.gov); Telephone: (515) 294-5606; FAX: (515) 294-8727

R. L. Terpstra

Metal & Ceramic Sciences Program, Ames Laboratory (USDOE),  
Iowa State University, Ames, IA. 50011, USA

E-mail: [terpstra@ameslab.gov](mailto:terpstra@ameslab.gov); Telephone: (515) 294-5747; FAX: (515) 294-8727

## Manuscript

### ABSTRACT

The use of metallic filters for trapping fine (1-20 $\mu$ m) particulate from hot (850°C) coal combustion exhausts can offer improved toughness and extended life over ceramic filters. Promising yield strength (200 MPa at 850°C), ductility, permeability, and corrosion resistance were obtained in porous (70% dense) samples that were vacuum sintered from tap-densified spherical powders of a Ni-Cr-Al-Fe alloy. To further improve the corrosion/oxidation resistance of the Ni-Cr-Al-Fe alloy, additional Al was added to enhance formation of the protective Al<sub>2</sub>O<sub>3</sub> scale and to increase the reservoir of Al for extended filter life. Two new Ni-Cr-Al-Fe alloys consisting of up to three times the Al content, relative to the base Ni-Cr-Al-Fe alloy, were developed and tested. The corrosion resistance of these aluminum-enriched alloys was evaluated, in both "as-received" and "pre-oxidized" conditions, utilizing an oxidizing/sulfidizing gas environment designed to simulate a typical pressurized fluidized bed combustion (PFBC) process. An asymmetrical four-point bend (AFPB) test was used to determine the yield strength of these alloys, in cast form, at room temperature, 600° C, and 850° C. Based on the results obtained, a Ni-Cr-Al-Fe alloy containing twice the aluminum content as the Ni-Cr-Al-Fe base alloy was selected as a viable filter alloy and was atomized using the Ames Laboratory high pressure gas atomizer for the purpose of further testing in filter form. The Ni-Cr-2xAl-Fe powder was sieved to the desired size of 25 – 45 microns and sintered to produce 0.5 mm thick porous sheets. Resistance welding trials were performed on the porous Ni-Cr-Al-Fe and Ni-Cr-2xAl-Fe sheets, tracking microstructural changes in the heat-affected zone (HAZ) of the weld due to different welding conditions. The successful outcome of this work resulted in the ability to produce a resistance spot welded porous cylinder of the Ni-Cr-2xAl-Fe alloy, suitable for extended exposure tests in a PFBC facility.

### INTRODUCTION

The pressurized fluidized bed combustion (PFBC) process has been developed to be a highly efficient, high-temperature combustion technique to burn coal containing high levels of sulfur. Unfortunately, a

major barrier to the implementation of the PFBC process has been the design of a robust hot gas filter material that possesses adequate corrosion resistance.[1] The filter must remove abrasive/corrosive “flyash” particulate from the hot (typically about 850°C) oxidizing/sulfidizing combustion gas to protect the gas turbine generator located downstream of the PFBC combustion zone. Initially, an array of multiple ceramic cylindrical “candle” filters was adopted to provide a copious amount of filtration area. However, the current ceramic filters appear to be too brittle to withstand typical operating conditions and procedures. [2,3,4] As a result, porous metal filters are being developed and considered as alternative devices to advance the PFBC process.

Generally, metallic materials used in PFBC applications will need to rely on the formation and preservation of a slow-growing  $\text{Al}_2\text{O}_3$  scale to protect the base metal from the surrounding environment. Formation of such an oxide scale is controlled by the diffusion kinetics between the aluminum constituent of the base alloy and the oxygen-bearing component in the combustion gas. To protect the base material, the oxide scale must react slowly with the surrounding environment and must form a continuous and adherent metallic oxide layer capable of enduring the effects of both growth and thermal stresses. [5] As the thickness of the oxide layer increases, it becomes significantly less strain tolerant and prone to spallation due, for example, to growth defects and thermal stresses. Healing or reformation of the alumina scale can occur in the event of scale cracking or spallation if a sufficient amount of aluminum is available for oxidation at the alloy surface. However, the finite thickness of the alloy component places a practical limit on the reservoir of aluminum and, hence, on the duration of sustained alumina-scale growth. Eventually, the aluminum content in the alloy will deplete below a level necessary for chemical equilibrium between the alloy and the alumina scale. At this point, “chemical” breakdown of the alumina scale results and formation of less protective oxides of the base metal ensues. [6]

Metallic filters based on the  $\text{Fe}_3\text{Al}$  (iron aluminide) intermetallic compound have been well developed as an alternate material for the ceramic hot gas filters. Compared with SiC and  $\text{Al}_2\text{O}_3$  filter materials, the iron aluminide filters offer a slight improvement in strength and resistance to thermal shock at the anticipated PFBC operating temperature of 850°C. Unfortunately, the brittle properties of the iron aluminides at ambient temperature are similar to ceramics and their strength at 850° C is not sufficient to resist creep elongation. The Ni-Cr-Al-Fe filter material developed at Ames Laboratory appears to offer significant benefits over both the ceramic and iron aluminide materials. [1] The Ni-Cr-Al-Fe alloy has shown the ability to maintain a nearly equivalent resistance to corrosion as the iron aluminide in initial sulfidizing/oxidizing corrosion tests at 850°C for up to 1000 hours. Also, the 850°C yield strength of the porous sintered Ni-Cr-Al-Fe material was observed to be at least 6 times that of the iron aluminides, while maintaining excellent room temperature ductility. [1]

Based on the results of previous studies, the premise of this study was that the service life of a metallic hot gas filter could be extended if sufficient aluminum were available for oxidation. Thus, this study investigated the influence of increasing the aluminum content of the Ni-Cr-Al-Fe alloy that was previously studied. Corrosion resistance to simulated PFBC operating conditions for 1000 hours and yield strength over a range of temperatures were observed as the aluminum content was increased up to three times the base Ni-Cr-Al-Fe alloy. This study also investigated the potential of resistance spot welding and forming thin (0.5 mm) porous sintered sheets into welded cylindrical shapes for further testing.

## RESULTS AND DISCUSSION

### Corrosion Tests

A high-temperature corrosion testing system was used to assess the long-term scaling resistance of the chill-cast candidate alloys containing 2 and 3 times more aluminum content than the base Ni-Cr-Al-Fe alloy. The base and modified alloys were tested in both the “as-received” and a “pre-oxidized” conditions. Pre-oxidation consisted of exposing the alloy sample to flowing argon gas for 50 hrs. at 1000° C. The purpose of the pre-oxidation treatment was to facilitate the formation of slow growing alumina as a continuous scale, preferably between 1 – 4  $\mu\text{m}$ , thick to protect the base metal before being exposed to the oxidizing/sulfidizing test environment. To reproduce the typical PFBC oxidizing/sulfidizing combustion environment, samples were exposed to a flowing  $\text{N}_2 - 13 \text{CO}_2 - 10 \text{H}_2\text{O} - 4 \text{O}_2 - 250 \text{ ppm SO}_2$  (in vol.%) gas mixture at 850° C for 1,000 hours. The samples were cooled to room temperature every 250 hours to record their weight change.

Figure 1 shows the comparison in the weight-change behavior of the reference Ni-Cr-Al-Fe alloy and  $\text{Fe}_3\text{Al}$  alloy in the as-received and pre-oxidized (“pre-ox”) conditions. As shown, the weight change of the as-received Ni-Cr-2xAl-Fe alloy, having twice the aluminum content as the reference Ni-Cr-Al-Fe alloy, is approximately half that of the as-received base alloy. By adding molybdenum to the 2xAl alloy, the weight change observed during this test was less than that of commercially available  $\text{Fe}_3\text{Al}$  alloy. The influence of the pre-oxidation treatment relative to the as-received sample condition is also shown in Figure 1. As can be seen, the pre-oxidized samples underwent significantly less weight gain than all of the as-received samples for the entire test period.

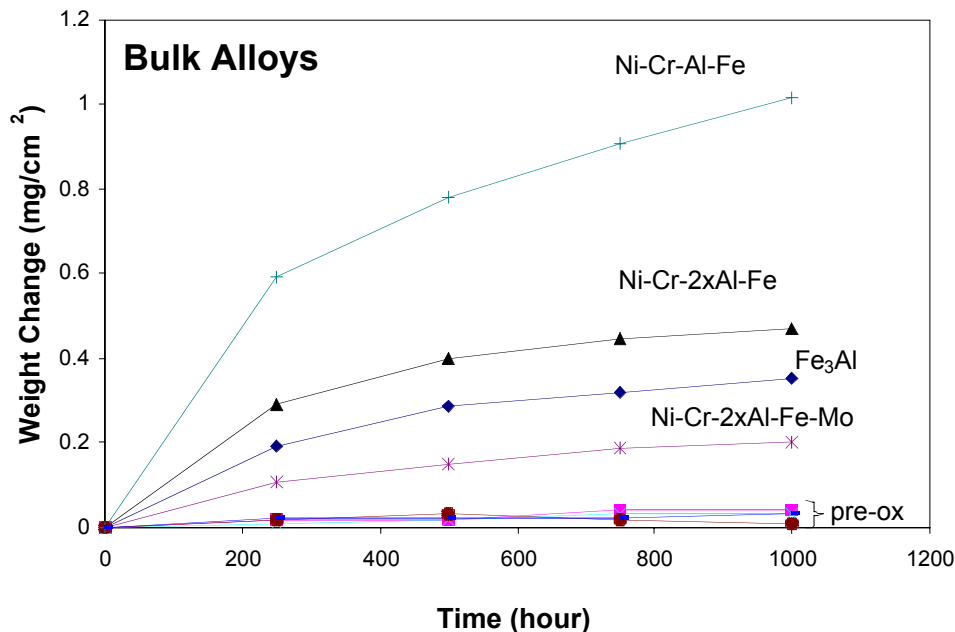


Figure 1. Corrosion test results of pre-oxidized and as received bulk alloys exposed to  $\text{N}_2-13\text{CO}_2-10\text{H}_2\text{O}-4\text{O}_2-250 \text{ pm SO}_2$  (vol. %) gas for 1000 h at 850° C.

The weight-change kinetics of the pre-oxidized samples is more clearly shown in Figure 2. As can be seen in this figure, the weight change for the pre-oxidized alloys is very small and there is little difference in the corrosion resistance under the conditions tested. As suggested earlier, if the aluminum within the alloy is the sole source for sustaining alumina-scale growth, then the more aluminum that is

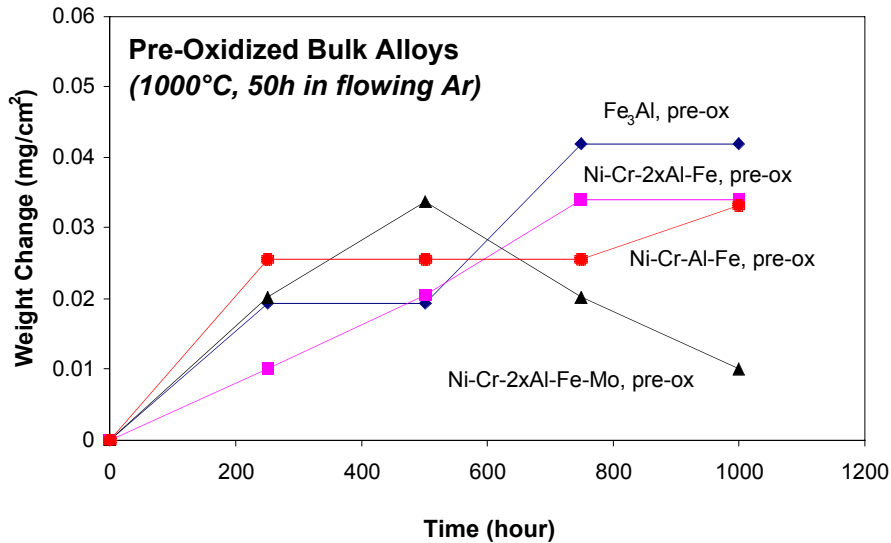


Figure 2. Corrosion test results of pre-oxidized bulk alloys exposed to  $N_2$ -13 $CO_2$ -10 $H_2O$ -4 $O_2$ -250 ppm  $SO_2$  (vol. %) gas for 1000 hrs. at 850° C.

available in the alloy, the longer the filter material should survive by prolonging chemical breakdown of the alumina scale. Based on this premise and the demonstrated beneficial influence of the “pre-oxidation” treatment, the possibility of increasing the corrosion resistance of an alloy should be achieved with an alloy that has a high aluminum content and is pre-oxidized. It should be noted, however, that weldability and toughness constraints place a practical limit on the amount of aluminum that can be added to the alloy. That limit was found to be approximately three times the amount in the Ni-Cr-Al-Fe base metal. Accordingly, results will be presented for only the 2xAl and 3xAl alloys, together with the base alloy.

Figure 3 shows the weight-gain kinetics for the modified alloys tested in the as-received and pre-oxidized states. The best performing alloy is seen to be pre-oxidized 2xAl. Interestingly, the 2xAl alloy performed better than the 3xAl alloy, either with or without pre-oxidation. This may be associated with the 3xAl alloy being overly brittle and consequently resulting in a greater frequency of scale cracking events, particularly during cooling after every 250 h of testing.

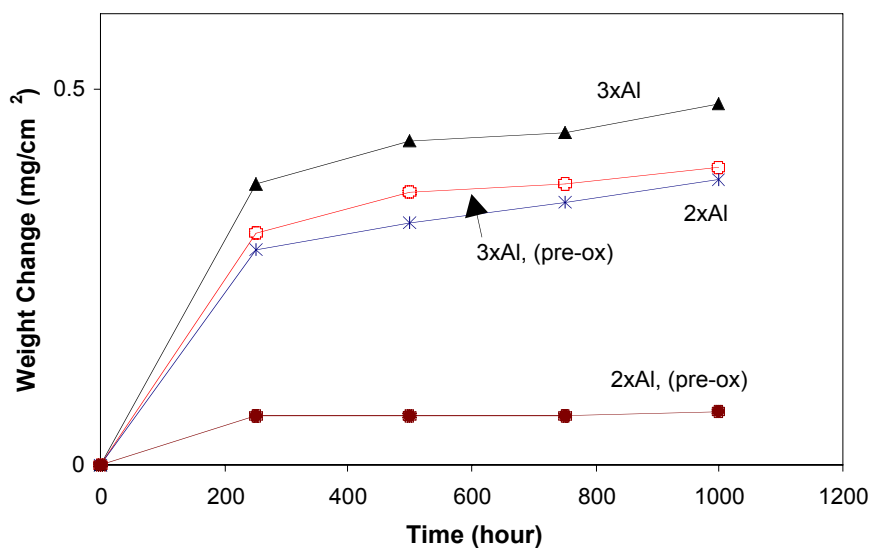


Figure 3. Corrosion test results of aluminum-enriched Ni-Cr-Al-Fe alloy ingots exposed to  $N_2$ -13CO<sub>2</sub>-10H<sub>2</sub>O-4O<sub>2</sub>-250 ppm SO<sub>2</sub> (vol. %) gas for 1000 hrs. at 850° C.

The superior corrosion performance of the pre-oxidized 2xAl alloy ingot prompted the atomization of the 2xAl alloy into powder. To simulate a metal filter element, gas atomized powder of the Ni-Cr-2xAl-Fe alloy, sized  $25\ \mu\text{m} < \text{dia.} < 45\ \mu\text{m}$ , was sintered to approximately a 70% density and exposed to the environmental test condition previously described. Figure 4 shows the weight-change results for both the as-received and the pre-oxidized cast and porous compacted samples. As can be seen, the weight change experienced by the porous sample was significantly higher than the ingot sample, primarily due

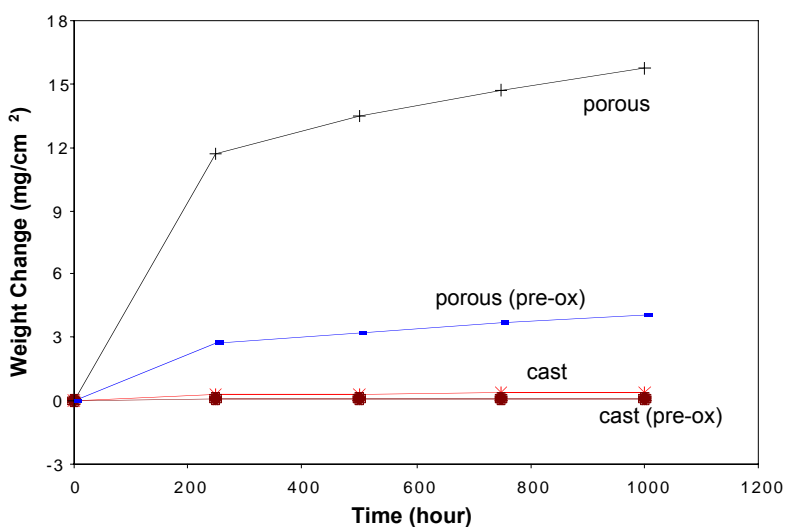


Figure 4. Corrosion test results of Ni-Cr-2xAl-Fe as cast and sintered porous samples to  $N_2$ -13CO<sub>2</sub>-10H<sub>2</sub>O-4O<sub>2</sub>-250 ppm SO<sub>2</sub> (vol. %) gas for 1000 hrs. at 850° C.

to the increased surface area of the porous sample exposed to the corrosive gas (*i.e.*, only the gross dimensional surface area was considered for the porous sample). However, the pre-oxidizing treatment remained extremely beneficial for limiting the weight change of the porous sintered 2xAl sample, relative to the as-received porous sample.

Protecting the base metal from the corrosive gas environment can be accomplished or at least minimized by forming a continuous alumina scale between the base metal and the corrosive gas. With continued alumina growth, the subsurface of the alloy becomes depleted in aluminum, eventually to the extent that internal oxidation of the aluminum and void formation may result. Such subsurface degradation is the precursor to breakdown of the protective alumina scale. Figure 5 shows cross-sectional SEM micrographs of various pre-oxidized samples after 1000 h testing. The 2xAl alloy is seen to form a thin, continuous scale layer with no clear evidence of subsurface degradation. The 3xAl alloy also developed a protective scale; however, rectangular internal precipitates in the vicinity of the alloy/scale interface were evident. It is inferred from rectangular morphology of these precipitates that they are the aluminum nitride, AlN. [7] Apparently, increasing the aluminum content in the alloy increases the preferential reactivity of aluminum to nitridation. The SEM image of the sintered powder, shown in Fig. 5c, reveals that a continuous protective oxide layer develops on powders of sufficient size and that the oxide layer does not jeopardize the inter-particle bond developed during the sintering cycle. However, powders less than about 15  $\mu\text{m}$  in diameter had a limited reservoir for sustaining alumina scale growth throughout the 1000 h test, as indicated by the fact that such powders underwent extensive attack (*i.e.*, some were through-corroded).

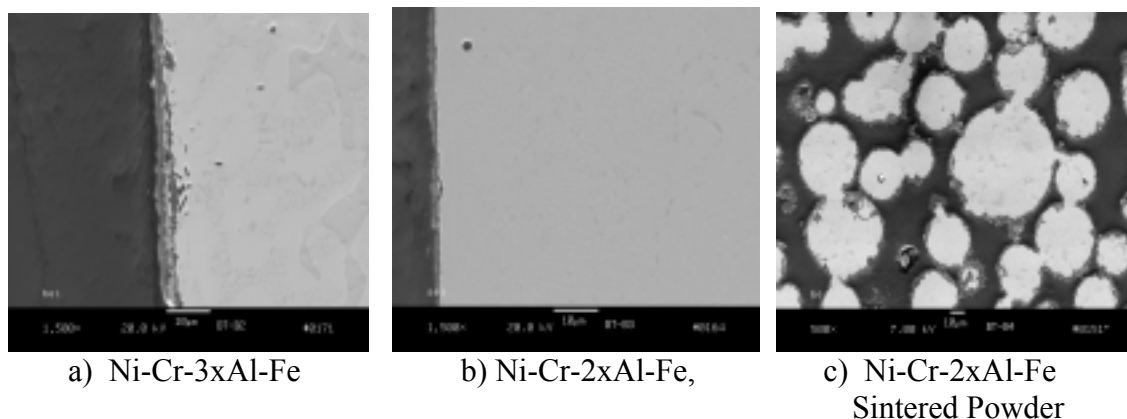


Figure 5. Cross sectional SEM images of pre-oxidized samples.

#### Yield Strength Results:

Figure 6 illustrates the yield strength, using an asymmetric four point bend (AFPB) test procedure and a strain rate of 0.1 mm/min., of several currently used and potential hot gas filter materials tested in air over a range of typical operating temperatures. As shown in the figure, the porous ceramic materials, Al<sub>2</sub>O<sub>3</sub> and SiC, demonstrated a very low, yet consistent yield strength for all the temperatures tested. A yield strength rise can be noted at 600° C for the Ni-Cr-3xAl-Fe chill-cast sample, perhaps due to a pronounced precipitation hardening effect promoted at the test temperature. Comparing the bulk samples, the Ni-Cr-2xAl-Fe alloy exhibited the highest yield strength at both room temperature and at 850° C. At this temperature, all of the alloys, including the porous Ni-Cr-Al-Fe sample, demonstrated

equal or higher yield strengths than the Fe<sub>3</sub>Al alloy. Also notable is that at 850° C, the yield strength of the Ni-Cr-2xAl-Fe is nearly approximately twice that observed for the Ni-Cr-Al-Fe alloy.

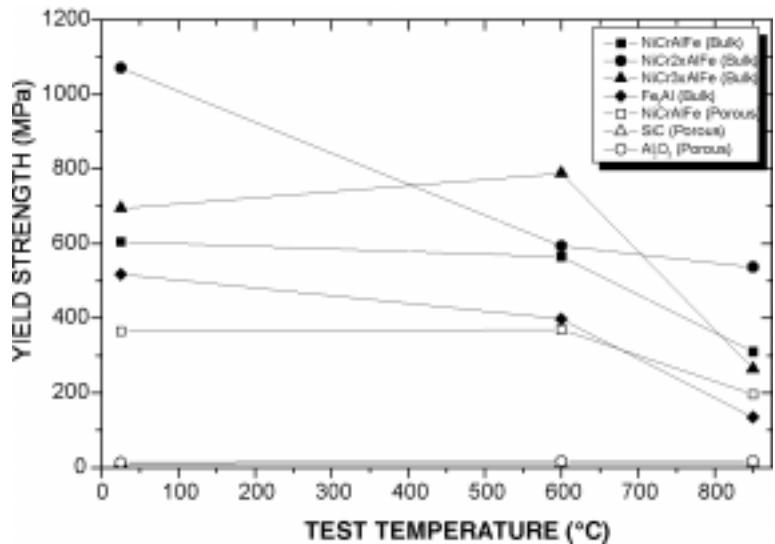
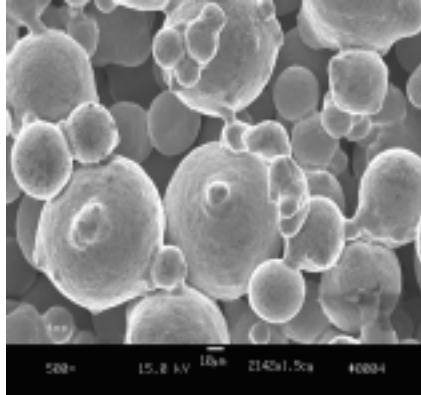


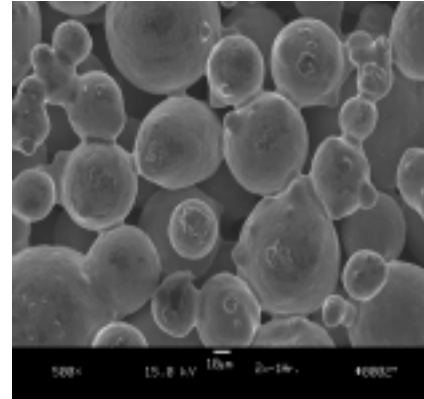
Figure 6. AFPB yield strength results.

Sintering Tests:

The corrosion results and the yield strength data verified the selection of the Ni-Cr-2xAl-Fe alloy for extensive development and testing of porous filter sheet material. Preliminary indications of brittleness for porous sheets of this alloy were eliminated by employing an extended sintering cycle to promote an enhanced state of bonding between sintered particles, as shown by comparing the SEM micrographs in Figure 7a and 7b. The extended sintering cycle maintained the simplicity of the sheet bonding process, without the need for post-sintering heat treatment. With this sintering method and an alumina mold, having a cavity of 3.8 mm x 25.4 mm x 0.5 mm, large porous sheet samples could be successfully produced without the aid of a mold release coating, where slight sintering shrinkage permitted mold release. The resulting 0.5 mm thick porous sintered sheet samples were rolled to a diameter equal to the outside diameter of a typical candle filter, verifying that the ambient temperature ductility of the porous material was sufficient for this application.



a) 0.5 hr. @ 1250° C

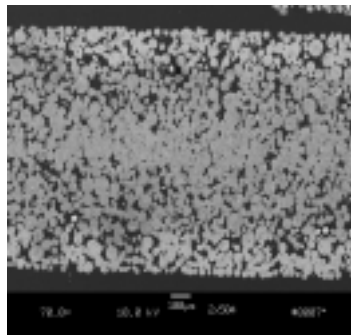


b) 1.0 hr. @ 1250° C

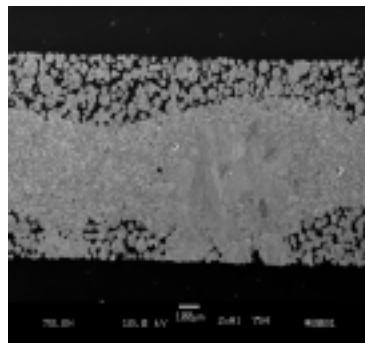
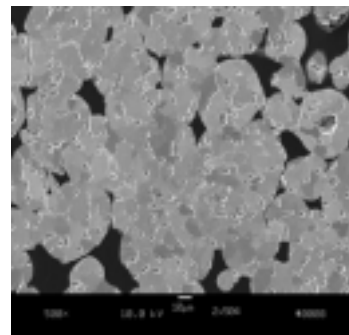
Figure 7. SEM images of sintered Ni-Cr-2xAl-Fe powder, 25 μm > dia. < 45 μm.

Resistance Spot Welding:

Resistance spot welding trials were conducted on the 0.5 mm thick strips of porous sintered Ni-Cr-2xAl-Fe material using a 20kVA resistance seam welder, Black & Webster model SWHD 850, converted to a resistance spot welder. There are several factors that influence a spot weld process. Figure 8 shows cross-sectional micrographs of resistance spot welds formed in this study using weld power levels of 10 and 15 kVA while maintaining a consistent total weld time of 66 ms. As shown, the welds formed using these 2 power setting resulted in weld zones having different microstructures. The weld re-solidification zone produced using the 10kVA setting appears to have developed a fine equiaxed grain size with some



a)



b)

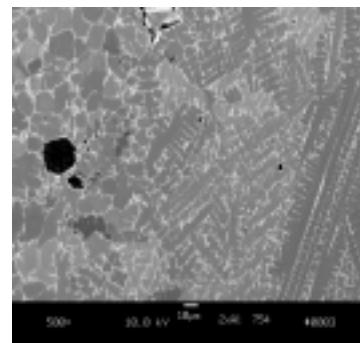


Figure 8. SEM images of Ni-Cr-2xAl-Fe resistance spot welds a) 10 kVA, b) 15 kVA.



apparent microvoids at the grain triple points. In contrast, more extensive fusion is evident in the 15 kVA weld of Figure 8b, where a partially dendritic re-solidification pattern developed. It is significant to note that both power levels produced welds that bonded the porous sheets from the interior contact surfaces, with exterior porosity remaining intact. This weld joint characteristic appears to have helped prevent cracking by distributing post weld stresses.

Figure 9 illustrates a 60.3 mm diameter rolled and welded “o-ring “ prototype filter sample, having a 0.5 mm wall. The prototype filter was fabricated using 25 < dia. <math><45\ \mu\text{m}</math> Ni-Cr-2xAl-Fe powder sample that was vacuum sintered to approximately a 70% density and joined using a series of resistance spot welds at 10 kVA for 66 ms. Having the ability to roll and weld the o-ring filter will allow porous sintered samples to be placed in a commercial PFBC system for long term corrosion testing and evaluation.



Figure 9. Resistance spot welded cylinder of porous sintered Ni-Cr-2xAl-Fe powder.

## CONCLUSIONS

Bulk corrosion resistance (weight change) of the Ni-Cr-Al-Fe alloy can be improved to become comparable to the corrosion resistance of the commercially available  $\text{Fe}_3\text{Al}$  alloy for use in a PFBC system through selective alloy design. Based on corrosion resistance and yield strength observations, doubling the aluminum content of the alloy was more beneficial than increasing the aluminum content in the alloy by a factor of three or four. Further improvements in the corrosion resistance of the Ni-Cr-2xAl-Fe alloy, however; may be needed to enhance the service life of actual hot gas filters. With respect to the manufacturing of metallic hot gas filter, doubling the alloy aluminum content was shown to not significantly impair the sintering or ductility of a thin porous sintered sheet. The Ni-Cr-2xAl-Fe alloy also demonstrated the ability to be joined using conventional resistance spot welding techniques. This will become particularly important when joining end caps and termination flanges to thin-walled metallic filters for in-situ prototype testing planned for at a later stage of this project.

## ACKNOWLEDGEMENT

Support from DOE-Fossil Energy through Ames Lab contract no. W-7405-Eng-82 is gratefully acknowledged.

## REFERENCES

1. Terpstra, R. L., Anderson, I. E., B. Gleeson (2001), "Development of Metallic Hot Gas Filters," in *Advances in Powder Metallurgy and Particulate Materials*, MPIF-APMI, Princeton, NJ, Vol. 8, (2001) p.84.
2. Oakley, J.E., Lowe, T., Morrel, R., Byrne, W. P., Brown, R., and Stringer J., *Materials at High Temperatures*, 14, (1997) p. 301.
3. Oakley, J.E., Lowe, T., Morrel, R., Stringer, J., and Brown, R., in Proc. 2<sup>nd</sup> International Conference on Heat-Resistance Materials, K. Natesan et al. (eds.), ASM International, Materials Park, OH, (1995) p. 537.
4. Alvan, M. A., in Proc. 2<sup>nd</sup> International Conference on Heat-Resistant Materials, K. Natesan et al. (eds.), ASM International, Materials Park, OH, (1995) p. 525.
5. Gleeson, B., "High-Temperature Corrosion of Metallic Alloys and Coatings," in *Corrosion and Environmental Degradation*, Vol. II: Volume 19 of the Materials Science and Technology Series, ed. M. Schutze (Weinheim, Germany: Wiley-VCH), (2000) p. 173.
6. Quadackers, W.J., Bennett M.J., *Mater. Sci., Technol.*, 10, (1994) p. 126.
7. Lai, G.Y., *High-Temperature Corrosion of Engineering Alloys*, ASM International, Materials Park, OH, (1990) p.82.